Isochronous Mass Spectrometer for Space Plasma Applications

P. Wurz, L. Gubler, and P. Bochsler

Physikalisches Institut, University of Bern, Bern, Switzerland

E. Möbius

Institute for the Study of Earth, Oceans and Space, University of New Hampshire, Durham, NH, USA

We have developed a new isochronous mass spectrometer and achieved high geometric factor and high mass resolving power, significantly exceeding the capabilities of isochronous spectrometers currently in use for the analysis of space plasmas. Ions with energies up to about 60keV can be detected. In combination with an electrostatic energy analyzer, the instrument will be used for measurements of the elemental, isotopic, and molecular composition of space plasmas. The instrument is of cylindrical geometry, therefore 3-dimensional velocity distributions of ions can be measured from a spinning spacecraft. We compare the performance of our instrument with those isochronous mass spectrometers currently in use on the WIND and SOHO spacecrafts.

1. INTRODUCTION

In carbon-foil time-of-flight (TOF) mass spectrometers (MS) a particle is identified by having it pass a thin carbon foil (≈100Å) to produce a start signal and then measuring the elapsed time until the particle hits a stop detector at a given distance. Knowing the energy of the particle, its mass can be inferred from the flight time.

In an isochronous TOF MS, ions travel in a suitably configured electrostatic field, where the flight time solely depends on the mass/charge (m/q) independent of the initial conditions of the ions. Only the fraction of the incident particles emerging from the carbon foil as ions can be used. Independent of the initial charge state, the majority of particles leaves the carbon foil neutral or as singly charged ions, because of efficient charge-exchange during passage through the foil [*Hvelplund et al., 1970; Bürgi et al., 1990; Gonin et al., 1992*]. Neutral particles are not deflected by the electrostatic field, and leave the isochronous TOF section. Since multiply charged ions are rare at the energies considered, the m/q spectrum consists mainly of singly charged ions and thus corresponds largely to a pure mass spectrum.

Within the TOF section of an isochronous instrument, ions are reflected back to the entrance plane by an electrostatic field increasing linearly along the z-direction, which is perpendicular to the entrance plane. The electrostatic field is derived from a quadratic potential. The motion of the ion along the linearly increasing field is a harmonic oscillation with a period independent of initial conditions such as initial energy or entrance angle. The TOF of an ion is only proportional to the square root of m/q.

Ideally, the resolution is only limited by the resolution of the time measuring system. This was successfully demonstrated in the laboratory by *Yoshida [1986]*. For space applications, mass resolutions of 100 and more can be reached when the geometry of the electric field is close to ideal. However, realizations of isochronous instruments so far either approximate the electric field to a limited degree [*McComas et al., 1990*] or use a configuration with an incomplete harmonic field combined with a linear TOF section [*Hamilton et al., 1990*]. The latter instrument, the so-called V-type MS, is currently in use on the WIND mission in the SMS/MASS sensor [*Gloeckler et al., 1995*] and on the SOHO mission in the CELIAS/MTOF sensor [*Hovestadt*

Measurement Techniques in Space Plasmas: Particles
Geophysical Monograph 102

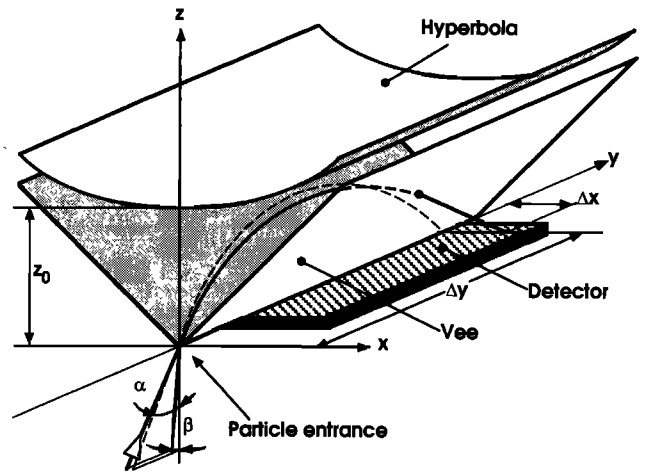

Figure 1. Schematics of a V-type isochronous mass spectrometer. The carbon foil is located at the particle entrance. Particles coming from a direction (α, β) move according to the electrostatic forces (solid line) until they exit through the vee. The dashed line is the projection of the trajectory on the yz-plane.

et al., 1995]. Recently, we introduced a new type of isochronous TOF MS with a cylindrically symmetric harmonic potential which allows an almost exact realization of the ideal field [*Gubler et al., 1995*]. Here we will compare the V-type and the cylindrically symmetric isochronous MS.

2. THE V-TYPE ISOCHRONOUS MASS SPECTROMETER

The underlying physical principle of the V-type MS is that the potential inside a quadrupole exhibits a quadratic behavior. Thus, one quadrant of such a quadrupole can serve as an isochronous MS. The V-type MS was first shown to work by *Hamilton et al.* [*1990*]. Figure 1 shows the schematics of the V-type instrument. The potential between the two electrodes (the hyperbola and the V-shaped ground plate, the "vee") is given by

$$\Phi(x,z)=\left(\Phi_0/z_0^{\,2}\right)\left(z^2-x^2\right)$$

with Φ_0 the voltage on the hyperbola and z_0 the separation of the hyperbola from the vee, which is electrically grounded. This configuration produces the desired field with the linear increase in z-direction.

To calculate the flight time we break the trajectory in two parts, $t_{TOF} = t_1 + t_2$, where t_1 is the flight time inside the harmonic potential and t_2 is the flight time from the vee to the detector. The trajectory inside the harmonic potential is derived by integrating the acceleration of the ion along its trajectory

$$v_x=\left(v_{0x}^{\,2}+x^2/t_0^{\,2}\right)^{\frac{1}{2}}\ ;\ v_y=v_{0y}\ ;\ v_z=\left(v_{0z}^{\,2}-z^2/t_0^{\,2}\right)^{\frac{1}{2}}$$

where v_{0x}, v_{0y}, and v_{0z} are the components of the initial velocity of the ion exiting the carbon foil at $x = 0$, $y = 0$, and $z = 0$, and using the abbreviation

$$t_0 = z_0\left[1/\left(2\Phi_0\right)\cdot\left(m/q\right)\right]^{\frac{1}{2}}.$$

Further integration along the trajectory in the quadratic potential leads to

$$x(t)=v_{0x}t_0\sinh\left(t/t_0\right)\ ;\ y(t)=v_{0y}t\ ;\ z(t)=v_{0z}t_0\sin\left(t/t_0\right)$$

The ion leaves the vee at a time t_1, which is where $x(t) = z(t)$. Thus we can calculate t_1 by solving

$$v_{0x}\sinh\left(t_1/t_0\right)=v_{0z}\sin\left(t_1/t_0\right)+\left(x_0/t_0\right)\cosh\left(t_1/t_0\right) \quad (1)$$

with x_0 being the start location. After leaving the vee, the flight time t_2 of the ion in the field-free area between the vee and the detector, located at $z = 0$, is

$$t_2=-z(t_1)/v_z(t_1)=t_0\tan\left(t_1/t_0\right)$$

For $\beta = 0$, with $\tan(\beta) = v_{0x}/v_{0z}$, and $x_0 = 0$, the solution of eq. 1 is trivial and we get $t_{TOF} = \pi t_0$. The flight time depends only on the m/q ratio and a constant instrumental parameter, independent of the initial energy of the ion.

In the following we will investigate the case for $\beta \neq 0$ and for $x_0 \neq 0$. For that purpose we have to solve eq. 1, which is possible only numerically, and the resulting flight time depending on β and x is displayed in Figure 2. It is obvious that the flight time becomes longer for increasing β. Starting from a location $x_0 \neq 0$ makes this deviation even worse.

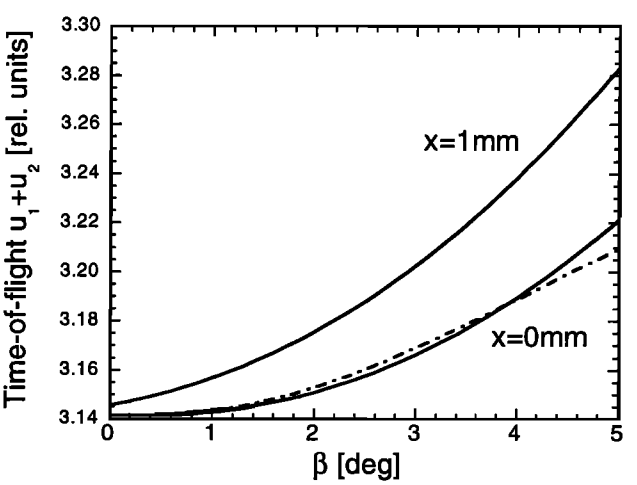

Figure 2. Dependence of TOF, $u_1 + u_2$, on the angle β for V-type instrument by numerically solving eq. 1 and calculating the total flight time for $x_0 = 0$ and $x_0 = 1$mm. Furthermore, the result from eq. 2 is shown (dashed-pointed line).

Therefore, the acceptance angle β of the detector has to be limited for sufficient time resolution. For the same reason the entrance area needs to be limited to small x_0.

To obtain an approximation for the deviation of the flight time from t_0, we expand the left-hand and right-hand sides of eq. 1 around $u_1 = \pi$ for $x_0 = 0$. Using the approximation $\sinh(t_1/t_0) \approx \exp(t_1/t_0)/2$ we get

$$u_1 \approx \pi - \frac{1}{2}\left(\beta e^{\pi} + 2\right) + \frac{1}{2}\sqrt{\left(\beta e^{\pi}\right)^2 + 4}$$

where we used the abbreviations $u_1 = t_1/t_0$ and $u_2 = t_2/t_0$. With $\tan(x) \approx x + x^3/3 + \ldots$ we get for the total flight time

$$t_{TOF} = t_1 + t_2 = t_0\left(u_1 + u_2\right) \approx$$
$$\approx t_0\left\{\pi + \frac{1}{3}\left[\frac{1}{2}\left(\beta e^{\pi} + 2\right) - \frac{1}{2}\sqrt{\left(\beta e^{\pi}\right)^2 + 4}\right]^3\right\} \quad (2)$$

The first and second order terms in u_1 and u_2 cancel out and the deviation of the flight time from t_0 is proportional to β^3. This is the reason why a V-type instrument has good mass resolution although the ions travel a considerable time in field free space. Up to $\beta = 5°$ this approximation is close to the exact result, which is shown in Figure 2. The flight time increases with β and x_0, and thus leads to an asymmetric appearance of the mass peaks, but is still independent of the initial energy and angle. Eq. 2 implies a theoretical limit for the mass resolution of a V-type instrument.

The mass resolution of a V-type instrument is determined by three contributions: the uncertainty of the TOF measurement, $\Delta\tau_e$; the theoretical limitations imposed by a spread in β and by x, $\Delta\tau_{\beta,x}$; and a term, $\Delta\tau_d$, because the detector cannot be placed directly in the $z = 0$ plane in a practical realization. Therefore, the mass resolution is

$$\frac{m}{\Delta m} = \frac{1}{2}\frac{t_{TOF}}{\Delta\tau} = \frac{t_{TOF}}{2}\left[\left(\Delta\tau_e\right)^2 + \left(\Delta\tau_{\beta,x}\right)^2 + \left(\Delta\tau_d\right)^2\right]^{-\frac{1}{2}} \quad (3)$$

The uncertainty of the TOF measurement, $\Delta\tau_e$, is a combination of the resolution of the electronics and the TOF dispersion of the start electrons. Due to the isochronous operation of a V-type instrument we can set $\Delta\tau_e/t_{TOF} \approx \Delta\tau_e/t_0$. This uncertainty is constant and does not depend on the particle's energy or mass.

The contribution from the second term in eq. 3 has already been discussed above. For the last term we have to evaluate the flight time differences for particles moving along a short linear TOF of length d_z with energies differing from the nominal energy E by $\pm\Delta E$

$$\Delta\tau_d = \frac{d_z}{4}\sqrt{\frac{2m}{E}}\left(\frac{\Delta E}{E}\right)_{C-foil} \approx \frac{d_z}{2\sqrt{2}}\frac{k_e}{E} \quad (4)$$

where ΔE is caused by the energy straggling in the carbon foil. In eq. 4 an approximation for the energy straggling is used [*Echenique et al., 1986; Beiersdorf et al., 1987*] with k_e being a constant. The energy resolution of the entrance system and the plasma temperature have to be folded into ΔE, which usually contribute only little for these instruments. Figure 3 shows the calculated mass resolution together with experimental results. The mass resolution scales linearly with z_0 through t_{TOF}, and is mainly limited by acceptance angle and entrance area. For low mass ions, limitations caused by $\Delta\tau_e$ become noticeable. In spite of these theoretical and practical limitations, the V-type instruments currently in use have sufficient mass resolution for isotope analysis at the price of overall detection efficiency.

The importance of the angular acceptance arises from the angular scattering of the ions in the carbon foil, in addition to the angular acceptance of the ion optical entrance system. The angular scattering in the carbon foil is substantial (about ±10°) for the ion energies in the range of keV/nuc [*Blokland et al., 1992*]. For good overall detection efficiency, the MS needs a large angular acceptance. For the V-type instrument, evaluation of the angular acceptance is straightforward. In y direction the instrument is built long enough to accept most of the scattered ions in α direction. In β angle the angular acceptance is constrained by the detector width. A trade-offbetween mass resolution and angular acceptance is necessary.

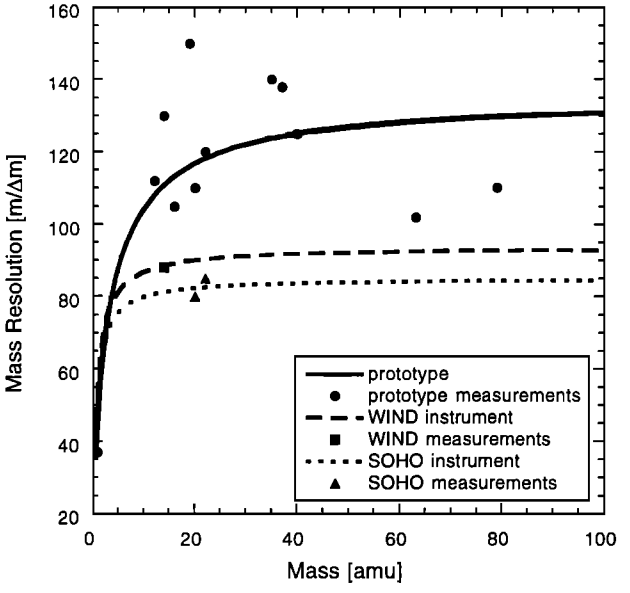

Figure 3. Mass resolution of V-type isochronous mass spectrometer as determined by eq. 3 for $\beta = 1.5°$, $\beta = 2.3°$, and $\beta = 3.0°$, using $z_0 = 5$cm and $\Phi_0 = 20$kV. Some experimental results are indicated: prototype [*Hamilton et al., 1990*], WIND [*Gloeckler et al, 1995*], SOHO [*Hovestadt et al., 1995*].

3. CYLINDRICALLY SYMMETRIC TIME-OF-FLIGHT INSTRUMENT

To extend the capabilities of isochronous MS and to overcome the limitations of the V-type instruments, we designed a cylindrically symmetric isochronous MS, which has been described in detail earlier [*Möbius et al., 1990; Gubler et al., 1995*]. The instrument is coined CYLMAS for CYLindrically symmetric MASs spectrometer, and has the same operation principle as outlined in the introduction.

The general solution of the Laplace equation for a quadratic potential in cylindrical geometry (r,ϑ,z) has the form

$$\Phi(r,z) = a + b\cdot\log(r/R) + (c/R^2)(2z^2 - r^2) \qquad (5)$$

where a, b, and c are free parameters and R is a fixed geometrical scale factor. The r-dependence is given by a quadratic and an additional logarithmic term. The quadratic component of the potential has a negative gradient in the r-direction and exerts a repelling force away from the center axis. As a consequence, ions are deflected outwards and may get lost. The attractive logarithmic component partly compensates for this defocusing effect. However, its effect decreases with increasing distance from the center axis.

Figure 4 shows the important parts of CYLMAS, realizing the potential given by eq. 5. Despite the rather complex r and z dependence only three electrodes are necessary, a lower, circular electrode, an upper cup, and a thin central rod. The cylindrically symmetric electrodes—the upper cup and the lower electrode—resemble equipotential surfaces and are on fixed voltages Φ_0 and Φ_u, respectively. The quadratically increasing potential along the central rod is generated by a special resistive coating, with the potential Φ_s at the footpoint and Φ_0 at the top. R is the radius of the active area of the detector (equal to the inner radius of the lower electrode), and r_s is the radius of the central rod. Inserting these parameters into eq. 5 leads to

$$\Phi(r,z) = \Phi_u + \frac{1}{2}\frac{\Phi_0-\Phi_u}{(Z/R)^2}\left\{1+2\left(\frac{z}{R}\right)^2-\left(\frac{r}{R}\right)^2+\right.$$
$$\left.+\left[2\left(\frac{Z}{R}\right)^2\frac{\Phi_s-\Phi_u}{\Phi_0-\Phi_u}+\left(\frac{r_s}{R}\right)^2-1\right]\frac{\log(r/R)}{\log(r_s/R)}\right\}$$

where we introduced an instrument parametrization by Z/R (see Figure 4), which is used to optimize the performance of CYLMAS. Independent of trajectory of the ion, we get for the flight time in the instrument

$$t_{TOF} = \pi Z\sqrt{\frac{1}{2(\Phi_0-\Phi_u)}\frac{m}{q}}.$$

For the mass resolution of CYLMAS we have to consider the uncertainty of the TOF measurement, and a second term, $\Delta\tau_f$, which accounts for non-ideal fields. Unlike the V-type instruments, there is no theoretical limitation for the mass resolution of the CYLMAS instrument, which is

$$\frac{m}{\Delta m} = \frac{1}{2}\frac{t_{TOF}}{\Delta\tau} = \frac{t_{TOF}}{2}\left[(\Delta\tau_e)^2+(\Delta\tau_f)^2\right]^{-\frac{1}{2}}$$

The limitation of the time resolution caused by $\Delta\tau_e/t_{TOF}$ is inversely proportional to Z and to the square root of the m/q because the total TOF scales with these parameters.

The potential distribution cannot be made perfect everywhere inside the instrument, which limits the mass resolution. The volume in front of the detector has been identified as the place, where the actual potential differs most from eq. 5 [*Gubler et al., 1995*]. We approximate this volume by a linear TOF section and thus we can use eq. 4 to derive $\Delta\tau_f$, with the path length d_z being the length of the non-ideal field region. The final result for the mass resolution is

$$\frac{m}{\Delta m} = \frac{\pi Z}{2}\left(\frac{1}{2}\frac{1}{(\Phi_0-\Phi_u)}\frac{m}{q}\right)^{\frac{1}{2}}\left(\Delta\tau_e^{\,2}+\frac{1}{8}\left(d_z\frac{k_e}{E}\right)^2\right)^{-\frac{1}{2}} \qquad (6)$$

Thus the mass resolution depends on three factors: it is proportional to Z and the square root of m/q, and it depends on an instrumental factor comprising the timing accuracy and the actual realization of the electrostatic field.

Calculating the angular acceptance of a cylindrically symmetric instrument is not as simple as for the V-type

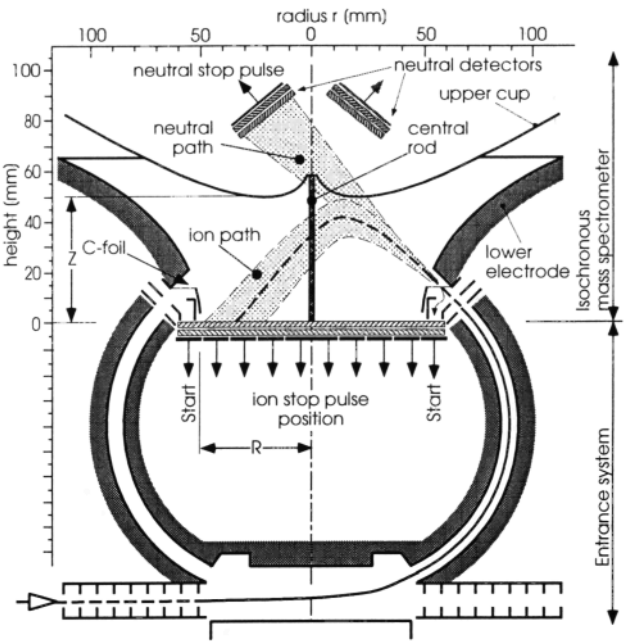

Figure 4. Schematic cross-section through the CYLMAS instrument showing the lower electrode, the upper cup, and the central rod.

instrument. Using the laws of conservation of energy and angular momentum in the $r\vartheta$-plane (the projection of the trajectory to the plane $z = 0$), an expression for the TOF for a given entrance radius, R, to the minimum radius, r_{min}, in the TOF-section is given by

$$T = \int_{R}^{r_{max}} \left(\frac{2}{m}\left(E_{r\vartheta} - q\Phi(r,0)\right) - \frac{P^2}{m^2 r^2} \right)^{-\frac{1}{2}} dr. \qquad (7)$$

P is the angular momentum of the ion moving in the $r\vartheta$-plane and $E_{r\vartheta}$ is the total energy of the ion in the $r\vartheta$-plane. Both P and $E_{r\vartheta}$ depend on the direction and energy of an ion at the point of entrance. For successful detection of an ion, the TOF in the isochronous direction z has to be shorter than twice the time T the particle needs to move from r_{min} to r_{max} in the $r\vartheta$-plane. If this condition is not met above $z = 0$, the particle has a theoretical impact location $r > R$ and hits the lower electrode instead of the detector. P is essentially determined by the entrance angle β, which is the azimuth angle. For $\beta = 0$ the trajectory aims at the center of the instrument. By varying the entrance angles α and β, where α is the elevation angle, the angular acceptance of CYLMAS is calculated and expressed as a solid angle. The angular acceptance depends on Z/R and on E/q with respect to Φ_0. Eq. 7 is evaluated for the potential given by eq. 5, with and without the logarithmic term. The angular acceptance for both cases and the mass resolution are shown in Figure 5 as a function of the parameter Z/R. As can be seen, high mass resolution has the penalty of a reduced angular acceptance and therefore a smaller geometric factor, and vice versa. For practical applications a compromise has to be made. We built the CYLMAS prototype with the dimensions $Z/R = 1$ and $R = 5$cm. At $E/q = \Phi_0$, the calculated

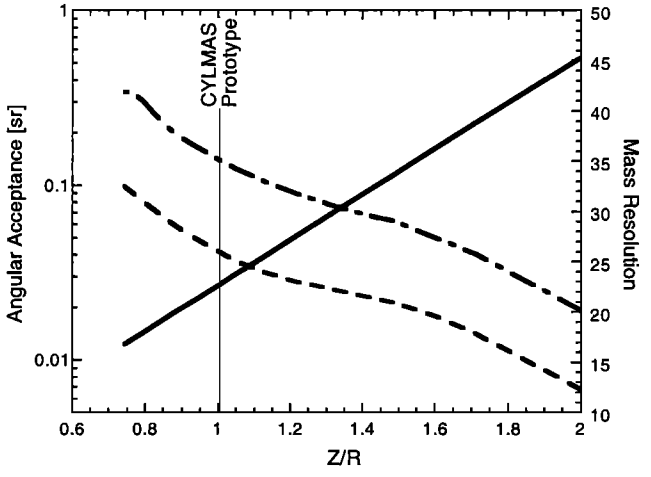

Figure 5. The angular acceptance for CYLMAS with (dashed-pointed line) and without (dashed line) the logarithmic term in the potential (eq. 5) and the mass resolution for hydrogen (solid line) are shown as functions of Z/R.

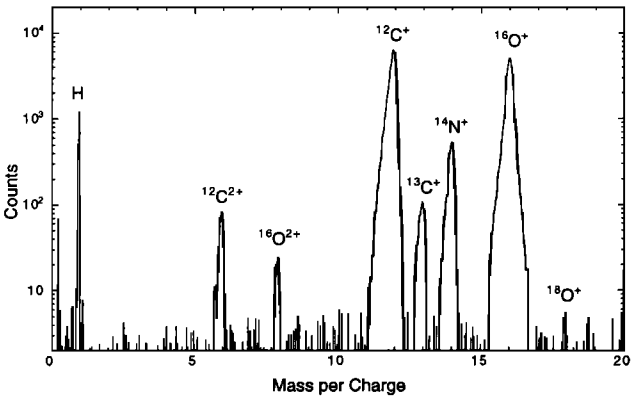

Figure 6. CYLMAS mass spectrum for the isochronous channel of a gas mixture of CO, N_2, and O_2 molecules. The spectrum (2048 points total) is smoothed (5-point-interval smoothing) and the background is subtracted.

angular acceptance is 0.15sr and 0.04sr, with and without the logarithmic potential, respectively. The higher value corresponds to 3 σ of the angular distribution after the carbon foil for particles with 20keV/nuc, which means that almost all ions reach the detector in this design. For $E/q < \Phi_0$ the angular acceptance increases substantially, but so does the angular scatter after the foil.

4. EXPERIMENTAL RESULTS

The CYLMAS prototype was exposed to an ion flux from a simple ion gun without mass filtering. The actual ion beam always contained a mixture of atomic and molecular ions (if a molecular gas was introduced) with a rate of approximately 1000 ions per second.

The CYLMAS instrument was mainly developed to demonstrate the capability to identify molecules with an isochronous MS. Since we discussed the identification of molecular ions before [*Gubler 1994; Gubler et al., 1995*], we will only discuss the performancefor atomic ions and the determination of isotopic ratios here.

Figure 6 shows a typical mass spectrum recorded with CYLMAS using a gas mixture of CO, N_2, and O_2. A beam energy of 40keV was used, and the voltage settings for the instrument are $\Phi_0 = 17.5$kV, $\Phi_u = -1.75$kV, and $\Phi_s = 0$V, which optimize the detection efficiencyfor molecules. Only positively charged fragments from molecules breaking up in the carbon foil can be analyzed. Incoming atomic ions were not repelled, because their energy was too high and they passed through the upper cup, which is realized as a grid. The mass resolution and the dynamic range in this operational mode allows the identification of the isotopes $^{13}C^+$ and $^{18}O^+$, as well as the doubly ionized species $^{12}C^{2+}$ and $^{16}O^{2+}$ after one hour of data collection.

The mass resolution of the CYLMAS instrument was determined from several measurements with various gas

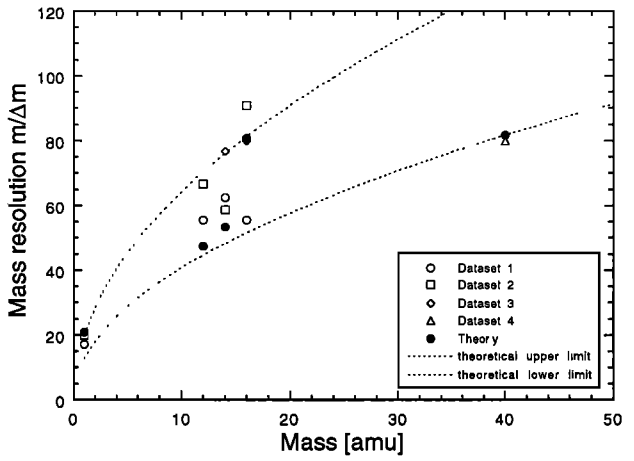

Figure 7. Comparison of the measured mass resolution for different masses with the theoretical mass resolution given by eq. 6. The different data sets are recorded with different beam energies (30–40keV). Theoretical values calculated with eq. 6 (dashed lines) are given for the lowest and highest beam energy used.

mixtures and various beam energies. For hydrogen, a mass resolution of 25 and for the heavier atoms C, N, and O a resolution of about 70 was achieved. If the parameters are optimized for atomic ions the mass resolution can be improved significantly. At $m/q = 12$ we obtained a the mass resolution of 160 [*Gubler et al., 1995*]. In Figure 7 the results of several measurements are compared with eq. 6. The mass resolution differs, because the measurements were performed at different beam energies. Eq. 6 predicts an energy dependence $m/\Delta m \propto E^{0.5}$, which is consistent with our measurements. The two dotted lines in Figure 7 represent the theoretical behavior given by eq. 6, for ions with 30 and 40keV, respectively, the highest and lowest energies used. All measurements are reproduced well by eq. 6, taking into account the energy loss in the carbon foil, with a value $k_e = 0.0298$eV s m^{-1} and the length of the non-ideal field of $d_z = 15$mm, which matches the gap between the lower electrode and the detector.

Even for molecular settings of the CYLMAS instrument, the mass resolution is sufficient to measure isotope ratios. For the $^{12}C/^{13}C$ ratio we obtain 1.3% (1.1%), for the $^{14}N/^{15}N$ ratio we obtain 0.38% (0.37%), and for the $^{16}O/^{18}O$ ratio we obtain 0.24% (0.20%), with the terrestrial values given in parentheses for comparison.

5. CONCLUSIONS

In cases when the resolution of isotopes and the unambiguous identification of molecules is needed an isochronous TOF MS has great advantages. The quadratic variation of the repelling potential, which leads to a harmonic motion and therefore to an excellent TOF focusing of the ion flight times, is achieved naturally with hyperbolic equipotential plates in a rotationally symmetric geometry. The addition of an attracting cylindrical potential in the center of the instrument partially overcomes the intrinsically divergent trajectories and improves detection efficiency. The efficiencies for different types of measurements are given in Table 1. The trade-off between resolution and detection efficiency has been discussed. The cylindrical symmetry allows a natural combination of this sensor with a toroidal top-hat analyzer for 360° acceptance of ions [*Sablik et al. 1988*]. This makes CYLMAS a natural candidate for the measurement of complete 3-dimensional ion velocity distributions, if operated on a spinning spacecraft. We have shown that in principle the cylindrically symmetric instrument is the better isochronous TOF MS, because of the improved angular acceptance and the larger active area compared to a V-type instrument. These improvements give rise to a significantly increased overall efficiency of CYLMAS over the V-type instrument, summarized in Table 2. In addition to the good mass resolution, which satisfies the requirements for isotope identification, the instrument has a very good collection efficiency for ions leaving the carbon foil with angular spreads of typically ±10°. Because the carbon foil ionization efficiency and the detection efficiency are multiplied for molecule detection, the overall detection efficiency of an isochronous MS, which is substantially higher for the CYLMAS design, becomes an extremely import figure of merit.

Table 1. Approximate detection efficiencies for the CYLMAS prototype for various types of measurements.

Type of measurement	Efficiency
TOF neutral channel	60%
TOF isochronous channel	10%
molecule: ion/neutral	0.5%
molecule: ion/ion	0.04%

Table 2. Comparison of the transmission for V-type and cylindrically symmetric isochronous mass spectrometers for $Z/R = 1$, without and with the logarithmic term in eq. 5.

Angular width (FWHM)	V-type TOF instrument	CYLMAS, without log.	CYLMAS, with log.
10 °	10%	60%	100%
20°	5%	40%	90%

Acknowledgments. The authors are grateful to J. Fischer, H. Hofstetter, and R. Liniger from the University of Bern for their contributions in the areas of design, fabrication and electronics, respectively, to R. Burkhalter and H. Schwab from the Ingenieurschule Biel, Switzerland, for their help in design and construction, and to K. Crocker, M. Granoff, and L.M. Kistler from the University of New Hampshire for their help in design and fabrication of the MCP detector of the isochronous channel. The work at the University of Bern was supported by the Swiss National Science Foundation. The work at the University of New Hampshire was partly funded under the NASA Contracts #NAS 5-31283 and #NAS 5-30613.

REFERENCES

Beiersdorf, P., A.L. Roquemore and R. Kaita, Characteristics of compact solid-target charge exchange analyzers for energetic ion diagnostics on tokomaks, *Rev. Sci. Instrum*, *58*, 2092–2098, 1987.

Blokland, A.A.E.v., T.W.M. Grimbergen and H.W.v.d. Ven, A mass-selective neutral particle anaylzer with background rejection, *Rev Sci Instrum.*, *63*, 1978–1987, 1992.

Bürgi, A., M. Oetliker, P. Bochsler, J. Geiss and M.A. Coplan, Charge exchange of low-energy ions in thin carbon foils, *J Appl. Phys.*, *68*, 2547–2554, 1990.

Echenique, P.M., R.M. Nieminen, J.C. Ashley and R.H. Ritchie, Nonlinear stopping power of an electron gas for slow ions, *Phys. Rev*, *A 33*, 897–904, 1986.

Hamilton, D.C., G. Gloeckler, F.M. Ipavich, R.A. Lundgren, R.B. Sheldon and D. Hovestadt, New high-resolution electrostatic ion mass analyzer using time of flight, *Rev. Sci. Instrum.*, *61*, 3104–3106, 1990.

Hovestadt, D., et al., CELIAS—Charge, Element and Isotope Analysis System for SOHO, *Solar Physics 162*, 441–481, 1995.

Hvelplund, P., E. Lægsgård, J.Ø. Olsen and E.H. Pedersen, Equilibrium charge distributions of ion beams in carbon, *Nucl. Instr. Meth.*, *90*, 315–320, 1970.

Gloeckler, et al., The solar wind and suprathermal ion composition investigation of the WIND spacecraft, in *The Global Geopsace Mission*, C.T. Russell (ed.), Kluwer Academic Publisher, 79-124, 1995.

Gonin, M., A. Bürgi, M. Oetliker and P. Bochsler, Interactions of solar wind ions with thin carbon foils—calibration of time-of-flight spectrometers, *ESA SP-348*, 381–384, 1992.

Gubler, L., *Isochrone Flugzeit-Massenspektrometer für den Einsatz im Weltraum*. PhD Thesis, University of Bern, Bern, Switzerland, 1994.

Gubler, L., P. Wurz, P. Bochsler, E. Möbius, High resolution isochrounous mass spectrometer for space plasma applications, *Int. J Mass Spect. 148*, 77-96, 1995.

McComas, D.J., and J.E. Nordholt, New approach to 3-D, high sensititvity, high mass resolution space plasma composition measurements, *Rev. Sci. Instrum.*, *61*, 3095–3097, 1990.

Möbius, E., P. Bochsler, A.G. Ghielmetti and D.C. Hamilton, High mass resolution isochronous time-of-flight spectrograph for three-dimensional space plasma measurements, *Rev. Sci Instrum.*, *61*, 3609–3612, 1990.

Sablik, M.J., D. Golimowski, J.R. Sharber, and J.D. Winnigham, Computer simulation of a 360° field-of-view "top-hat" electrostatic analyzer, *Rev. Sci Instrum.*, *59*, 146–155, 1988.

Yoshida, Y., Time-of-flight mass spectrometer, US Patent 4,625,112, 1986.

P. Bochsler, L. Gubler, and P. Wurz, Physikalisches Institut, University of Bern, Sidlerstrasse 5, CH-3012 Bern, Switzerland. (e-mail addresses: Bochsler@soho.unibe.ch; Lukas.Gubler@ubs.com; Wurz@soho.unibe.ch)

E. Möbius, Institute for the Study of Earth, Oceans and Space, University of New Hampshire, Durham, NH 03824, USA. (e-mail: Moebius@rotor.sr.unh.edu)